



Prediction of earthquake-induced permanent deformations for concrete-faced rockfill dams

Selda Durmaz¹ · Deniz Ülgen¹

Received: 5 March 2020 / Accepted: 11 September 2020 / Published online: 6 November 2020
© Springer Nature B.V. 2020

Abstract

Prior studies highlight the importance of earthquake-induced permanent displacement for the safety assessment of the embankment dams. Concrete-faced rockfill dams (CFRDs) have become popular at especially seismically active regions with their high seismic energy absorption capacity. However, seriously damaged rockfill dams have been reported after some earthquake exposures. Even so researchers have focused on the dynamic response of embankments, few studies have been conducted to reveal the seismic behavior of rockfill dams. In this study, the issue under scrutiny is to establish a preliminary design procedure considering the earthquake-induced permanent displacement and acceleration response of CFRDs. For this purpose, numerical models are prepared with various geometric and material properties. Real earthquake records are used for seismic excitation. Dynamic analyses are conducted with a finite element method-based software. The equivalent linear analysis procedure is followed under two-dimensional plain-strain condition. Acceleration responses of dams are recorded at the centerline of the models. Then, the Newmark's sliding block approach is utilized to calculate the permanent displacements from acceleration records. A procedure is developed for the engineers to foresee the likely permanent displacement at the preliminary design stage. To prove the reliability, the recommended procedure is applied to case histories, and then the results are compared.

Keywords Concrete-faced rockfill dam (CFRD) · Newmark's sliding block method · Permanent deformation · Equivalent linear analysis · Finite element method

1 Introduction

Concrete-faced rockfill dams (CFRDs) are mostly used dam types around the world (Marandi et al. 2012; Wang et al. 2017). Rockfill material is preferred because of its high seismic energy absorption capacity during the earthquake, and with the heights above 300

✉ Selda Durmaz
seldadurmaz_22@hotmail.com

Deniz Ülgen
denizulgen@gmail.com

¹ Department of Civil Engineering, Faculty of Engineering, Muğla Sıtkı Koçman University, 48000 Kötekli/Muğla, Turkey

m, this dam type can increase the energy production capacity. Moreover, the concrete face slab on the upstream bears the water pressure and prevents the leakage (Liu et al. 2016). Thus, this dam type is approved from all engineering perspective, and its application is increased around the world (Sherard and Cooke 1987). Since many of CFRDs are located at the regions with intensive seismic activity, seismic safety and dynamic response of these structures have vital importance (Liu et al. 2016).

In 1965, earthquake-induced permanent deformations of earthfill dams were firstly calculated by Newmark, and this method is known as Newmark's sliding block analysis (Newmark 1965). Makdisi and Seed (1978) and Hynes-Griffin and Franklin (1984) proposed that the sliding masses should be non-rigid, and Hynes-Griffin and Franklin (1984) suggested a 100-cm deformation limit for the embankments. Lin and Whitman (1986), Ambraseys and Menu (1988), Jibson (1993), Bray et al. (1995), Kramer and Smith (1997) focused on the Newmark's method. The assumptions of Newmark's original method were modified by the researchers. Studies yielded some equations, tables, and graphs for the calculations of permanent deformations. Leshchinsky (2018) noted that the conventional Newmark approach neglects the occurrence of multiple shear zones in the sliding part of the slope and suggested nested Newmark method (NNM). This nested Newmark method (NNM) divides the slope into a series of nested failure wedges with different yield acceleration and may lead to larger displacements than rigid sliding block procedures.

In addition to the deterministic methods, Jibson (2007), Bray and Travararou (2007), Rathje and Saygılı (2009) made probabilistic studies to consider the unpredictable nature of seismic excitations. They also emphasize on the importance of selection of the intensity measures (peak ground acceleration, PGA; peak ground velocity, PGV; Arias intensity, I_a). Although the Arias Intensity is mostly dictated parameter to represent the input motion among the measures, combination of these parameters is mostly recommended by the researchers (Bray and Travararou 2007; Wang 2012; Saygılı and Rathje 2008). According to Bray and Travararou (2007) and Saygılı and Rathje (2008), PGA is the most efficient parameter if the yield coefficient (k_y) is equal or more than 0.1, and Arias Intensity is the most efficient ground motion parameter for $k_y=0.05$. Associated with the development of dynamic procedures, permanent displacement analyses of fill dams are conducted by using finite element or discrete element-based software (Kramer and Smith 1997). Swaisgood et al. (2003) studied nearly 70 case histories of earth dams and embankments and then developed a numerical relation between the crest settlements, earthquake magnitude, peak horizontal ground acceleration and dam height. Further studies combine both numerical and probabilistic methods, and their results are compared with case studies. Singh et al. (2007) used the results of 122 case histories on the performance of earth dams and embankments during past earthquakes. Permanent deformations of these case histories were also calculated with some Newmark-based methods, and according to the comparison of calculated and observed results, in general, calculated ones are smaller than the real observations. Likewise, Meehan and Vahedifard (2013) reevaluated the results of 122 case studies of earth dams and embankments utilizing 15 suggested methods for the calculations. Comparisons indicated that the observed deformations were greater than the calculated ones. Liu et al. (2014) conducted a large-scale shaking table test on a CFRD prototype. The results of the analyses revealed that the crest settlement is greater in comparison with the other parts. Wang et al. (2017) conducted a large-scale shaking table test on concrete-rockfill combination dam models. According to the results, maximum displacements occur near the dam crest, the amplification factors in the upper portion of dam increase with height, and lower frequencies increase with increasing peak ground acceleration. Pang et al. (2018) used an incremental dynamic analysis (IDA)-based seismic fragility

analysis method to evaluate the seismic performance of high concrete face rockfill dams. They established some relations between the relative settlement ratio, damage index, failure probability, peak ground acceleration. The proposed method was verified with Zipingpu CFRD and literature, and the results were reasonable. Roy et al. (2016) carried out a parametric study to investigate the effects of ground motion parameters on permanent displacements of sliding soil mass. According to this study, the displacement increases with increasing Arias Intensity while decreasing with increasing duration of the motion. Wang et al. (2020) improved the Newmark method on the basis of machine learning and proposed a SS-XGBoost framework. The researchers introduced a computational tool including subset simulation (SS) and K -fold cross-validation (CV) procedures for a data-driven Newmark displacement prediction. The suggested framework is applicable for the cases including slope stability assessments, ground motion prediction and liquefaction assessment with a satisfying generalization ability. Huang et al. (2020) presented a configuration of Newmark and spectral element method (SEM) for the seismic assessment of the slopes on the regional scale. 3D wave field, complex topography and hydrogeological conditions are the important focus of interest in the study. The landslide modeling ability of the SEM method for a large-scale simulation as hundreds of kilometers is also emphasized.

Despite the CFRDs are distributed around the world especially seismically active zones and any dam failure at these earthquake-prone areas can lead fatal disaster, as mentioned above, available methods are mostly suggested for any embankments or earthfill dams, not only for rockfill dams. Available methods are still not enough to foresee the dynamic response of CFRDs. To minimize the earthquake-induced damages, engineers should have comprehensive knowledge of the preliminary design stage.

The main objective of this paper is to establish a preliminary design procedure for CFRDs. The present study covers a series of numerical analyses to investigate the dynamic behavior of CFRDs under earthquake excitation. According to the conducted analyses, the effects of maximum ground acceleration, geometric properties of dam and rockfill material parameters on the response of rockfill dams are observed. Some relations are established between the most efficient parameters and earthquake-induced permanent displacements. Besides, less effective factors on the variation of acceleration are determined. Since this study aims to provide some practical approaches prior to the final design of the CFRDs, the relevance of the outcomes of the numerical analyses is discussed utilizing the case histories. The displacements of the case studies are reevaluated from the proposed figures (Fig. 13). The yield acceleration of the dam (a_{yield}) and the maximum ground acceleration of the input motion (PGA) are the available and common parameters for both numerical models and case studies. Thus, the displacement data of 37 cases observed at the site after earthquake exposure and the displacement data of 37 cases inferred from the outcomes of the numerical analyses are compared on the basis of $a_{\text{yield}}/\text{PGA}$ ratio.

2 Validation of numerical modeling

Computer-aided software can sometimes yield incorrect results or be unable to simulate the problem properly. Therefore, software should be tested with a known case history. To check the modeling ability of QUAKE/W for the dynamic analysis of dams, Sürgü Dam is simulated firstly.

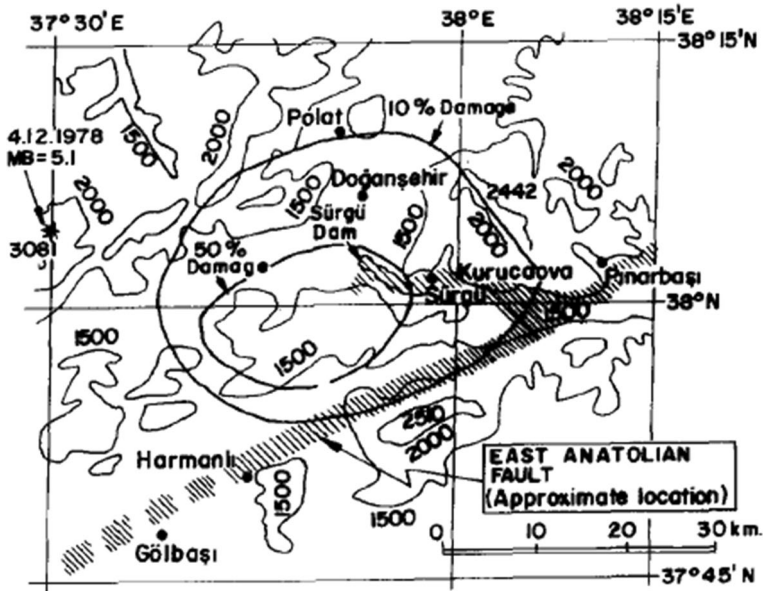


Fig. 1 Location of Sürgü Dam (Özkan et al. 1996)

Sürgü Dam was constructed on Sürgü stream of Malatya in southeast Turkey as seen in Fig. 1. This 55-m-high dam is a clay core type rockfill dam with a crest of 736 m length and 10 m width (Özkan et al. 1996). The impermeable core consists of sandy and silty clay, and weathered gneiss material is utilized for rockfill parts. There are different zones, and the details of dam cross section are illustrated in Fig. 2.

One of the major strike-slip fault mechanisms of Turkey, East Anatolian Fault, generated an earthquake with a magnitude of 5.8 (M_b) in 1986, and its epicentral distance was 10 km. According to the report of Özkan et al. (1996), the width of longitudinal cracks on the crest reached 20 cm and the maximum elongation of a continuous crack was 150 m. Many cracks were observed around the upstream part with the depth of 0.5–3.0 m from the crest, and the settlement of the crest was about 15 cm.

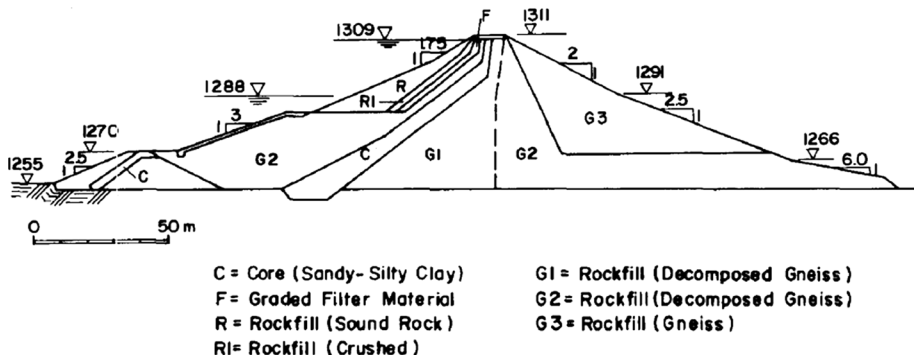


Fig. 2 Cross-section of Sürgü Dam (Özkan et al. 1996)

In the light of these data, a numerical model of Sürgü Dam was prepared in QUAKE/W to compare the numerical and measured results. Observed deformations due to the Malatya earthquake and outputs of QUAKE/W were compared. Thus, both algorithm of software and applicability of the Newmark method were examined for the case of seismic slope stability assessment of rockfill dams.

According to the partition in Fig. 2, a numerical model of Sürgü Dam was prepared in QUAKE/W with the given material properties in Table 1. As seen in the table, rockfill and transition materials are all gneiss, with different internal friction angles. The degradation curves for shear modulus and damping are provided from the study of Jia and Chi (2012). Illustrations of the proposed curves are given in Sect. 3.

Acceleration records of the Malatya earthquake were recorded at different stations; however, site conditions of available stations are not similar to the location of Sürgü Dam. Therefore, the input motion of the model was obtained from the earthquake database. The assessment of the seismicity of the site and the properties of the earthquake are given in the study of Özkan et al. (1996). According to assessments, potential PGA is defined as 0.15 g by the researchers. In the present study, potential of the East Anatolian Fault, records obtained from the nearest faults, fault type of the site, and the distance of the dam to the fault were considered during the selection of the earthquake records. The magnitudes of selected earthquakes were delimited between 5.0 and 6.0, and these earthquakes were generated by strike-slip fault coherently with East Anatolian Fault. Three different earthquakes were selected, and the acceleration records of each earthquake obtained from two different stations. Hence, the dam model was subjected to six different input motions. Taking into account of the dam site and the closest fault, the epicentral distance was determined as 10 km. The tabulated form of the used input motions is given in Table 2.

Table 1 Material properties of Sürgü Dam (Özkan et al. 1996)

Material type	Internal friction angle (°)	Cohesion (kN/m ²)	Poisson's ratio	Dry unit weight (kN/m ³)
Core (C) (sandy and silty clay)	22	10	0.42	19.5
Rockfill (G1) (decomposed gneiss)	27	0	0.30	19.5
Rockfill (G2) (decomposed gneiss)	33	0	0.30	19.5
Rockfill (G3) (gneiss)	35	0	0.30	19.5
Rockfill (sound rock)	40	0	0.30	19.5
Filter	33	0	0.38	19.5

Table 2 Earthquakes used in Sürgü Dam analyses

Earthquake	Moment magnitude	Arias intensity (m/s)	Epicentral distance (km)	PGA (g)	Fault mechanism	Duration (s)
Coyote Lake-1	5.74	0.1	10.67	0.12	Strike-slip	26.83
Coyote Lake-2	5.74	0.5	9.02	0.26	Strike-slip	26.86
Mammoth Lakes-1	5.94	0.5	12.39	0.31	Strike-slip	25.995
Mammoth Lakes-2	5.94	1.0	12.39	0.38	Strike-slip	11.5
Parkfield-1	6.0	1.0	9.95	0.17	Strike-slip	60
Parkfield-2	6.0	1.0	9.34	0.20	Strike-slip	60

Static and dynamic analyses were conducted with the equivalent linear analysis option of QUAKE/W. As illustrated in Fig. 3, 409 finite elements were generated for the numerical model considering the previously mentioned wavelength limitations. The bottom supports of the dam models are fixed in X and Y directions; left and right sides are free for both the validation and numerical simulations. The location of the slip surface is clearly shown in the site reconnaissance of Özkan et al. (1996), so that the same location as the site could be observed in the validation. Although Özkan et al. (1996) noted the observed failure in slip surface 1, additional slip surfaces were randomly defined as shown in Fig. 4. QUAKE/W is unable to model multiple slip surface. Therefore, analyses were conducted individually and repeated for each slip surface. However, the given results belong to slip surface 1 for the comparisons of numerically evaluated and measured deformations.

Initially, earthquake-induced acceleration records in dam body and yield acceleration of slip surface 1 were obtained under different excitations. Then, the Newmark's sliding block analysis procedure was followed to calculate the earthquake-induced permanent displacements.

Acceleration amplifications through Sürgü Dam reached up 3 times of maximum ground acceleration during the Malatya earthquake. Likewise, maximum ground accelerations were amplified 2.5 times for the numerical simulation of Sürgü Dam. Variation of accelerations along the dam height is shown in Fig. 5.

Finally, permanent displacement values of slip surface 1 were obtained under six earthquake records. If 1 cm deformation is neglected due to its low Arias intensity, obtained deformations varied between 14 and 27 cm as given in Table 3. The reconnaissance of Özkan et al. (1996) stated 20-cm permanent displacement at Sürgü Dam after the Malatya earthquake.

Consequently, when the acceleration amplifications at dam crest and calculated permanent displacements of stated slip surface are compared with the measured ones, despite the minor differences, they are mostly compatible. The validation study of Sürgü Dam indicates the appropriateness of QUAKE/W for the dynamic analysis of fill dams.

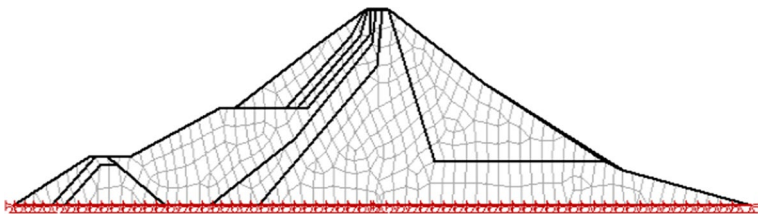


Fig. 3 Mesh generation of Sürgü Dam

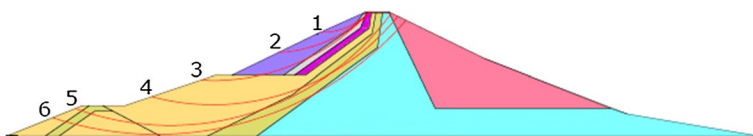


Fig. 4 Slip surfaces of Sürgü Dam

Fig. 5 Normalized acceleration variation through the dam body

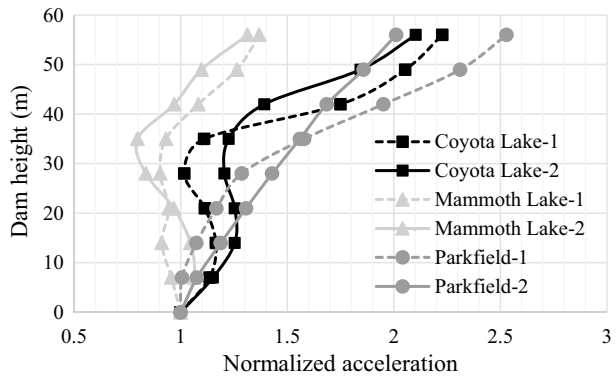


Table 3 Comparison of maximum permanent displacements

Earthquake	Evaluated maximum permanent displacement with QUAKE/W (cm)	Observed maximum permanent displacement at the site (cm)
Coyote Lake-1, 8/6/1979	1.00	20.00
Coyote Lake-2, 8/6/1979	14.00	
Mammoth Lakes-1, 5/27/1980	23.00	
Mammoth Lakes-2, 5/27/1980	27.00	
Parkfield-1, 9/28/2004	13.00	
Parkfield-2, 9/28/2004	27.00	

3 Numerical modeling

In this study, 1728 dynamic analyses consisting of different combinations of dam height (H), peak ground acceleration of the input motion (PGA), upstream and downstream inclinations, and six earthquake records were conducted. Dynamic analyses were carried out with the equivalent linear analysis option of finite element-based software QUAKE/W, under two-dimensional (2D) plain-strain conditions. Initial static stress distributions and earthquake-induced stresses are evaluated with this software. Unit weight, internal friction angle (Φ) and Poisson’s ratio (ν) of materials are required material parameters for QUAKE/W to calculate the stresses through the dam body. Poisson’s ratio is used to calculate the coefficient of earth pressure at rest condition (K_0), and this parameter is utilized to evaluate the mean effective stresses (σ'_m).

QUAKE/W computes the value of K_0 with the following equation:

$$K_0 = \frac{\nu}{1 - \nu} \tag{1}$$

Additionally, the mean effective stress is expressed as:

$$\sigma'_m = \frac{\sigma'_1 + \sigma'_2 + \sigma'_3}{3} \tag{2}$$

$$\sigma'_2 = \sigma'_3 = K_0 \times \sigma'_1 \tag{3}$$

This software provides three constitutive material models including linear elastic model, equivalent linear model and nonlinear model on the bases of the finite element method. The equivalent linear dynamic model can be used to simulate the dynamic loading included scenarios. As is known, repeated loadings change the dynamic properties of materials. QUAKE/W enables the definition of damping and modulus degradation curves, for the consideration of variation in shear strength and damping capacity of soil due to shock waves.

Application of the finite element method requires some discretization rules. As stated by Kuhlemeyer and Lysmer (1973), frequency content and velocity of incoming waves

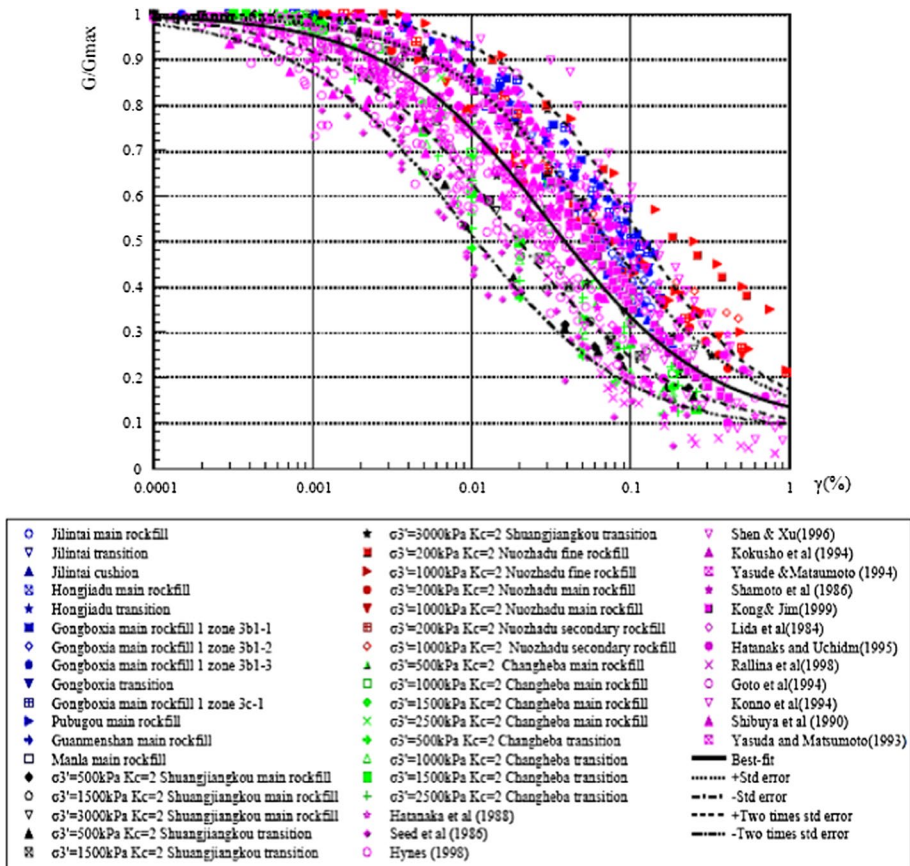


Fig. 6 Data points defining G/G_0 versus γ relationships for 35 kinds of rockfills based on testing along with the best-fit curve, \pm one standard division curves and two times standard division curves (Jia and Chi 2012)

play an important role in the calculations of finite element dimensions. A finite element size (ΔL) should be less than one-eighth or one-tenth of the wavelength with the highest frequency (λ). This limitation is considered during the mesh generation of the dam model, and one-tenth of the wavelength with the highest frequency is considered for the finite element size of the dam models.

When the anticipated strain level of the soil is very small for ascending stress, the linear elastic material model can be used. However, if the soil exhibits medium or high strains due to an increasing loading, nonlinear behavior conditions should be considered. Due to the nonlinearity of the soil, stiffness and shear modulus decrease, while the damping increases with increasing stresses. Nonlinear soil parameters are difficult to obtain, and nonlinear basis software takes longer time for calculations. Besides, the linear elastic approach is unable to model the effects of strain variations. The equivalent linear analysis combines these two methods, and nonlinear soil properties are utilized in a linear analysis calculation procedure. The linearization process includes iteration steps. Iteration starts with small strain values of shear modulus and damping and then continues until a certain convergence is satisfied. Thereby, effects of strain increment can be estimated in reasonable calculation time. Although the results of the equivalent linear analysis are overestimated, it is mostly used due to the fast computational ability.

Cyclic loading leads to variations in damping and shear modulus properties by causing strength loss in materials (Roy et al. 2016). As stated above, the equivalent linear procedure is followed for the numerical analyses of this study, and this procedure requires strain-dependent dynamic material properties to approximate the realistic response of materials. To consider the strain changes in rockfill, shear modulus and damping curves suggested by Jia and Chi (2012) were utilized (Figs. 6, 7). Their study considers strain dependency of 35 kinds of rockfill material, and the results are represented in terms of best-fit curve, one standard division curves and two times standard division curves. Best-fit curve is selected for this study.

Since this is a numerical study, rockfill material is assumed as a suitable type of material for dam construction and no specification is made for rock type. As summarized in Table 4, while generic values of the unit weight (γ), the Poisson's ratio (ν) and the cohesion (c) are used and kept constant for all models, internal friction angle was changed to investigate whether or not it has any influence on the dynamic behavior. According to ICOLD (2004) designation of the zonation for CFRDs, dam body includes similar granular rockfill material. These similar materials exhibit mostly similar dynamic behavior. Thus, effect of zonation is ignored, and dam bodies are simulated homogeneously. Uniformly modeled dams give acceptable and logical results. Furthermore, since there are many parameters to be examined, the effects of water, concrete slab and foundation are ignored for the sake of the study.

Dynamic loadings of the models were supplied from real earthquake records. Horizontal components of six different earthquakes were selected. Applied accelerograms belong to the earthquakes which were generated by different fault mechanisms and had different frequency content. The moment magnitude range was preferred from 6.5 to 7.5. Used earthquakes are summarized in Table 5 with time series and response spectra in Figs. 8 and 9, respectively. This study intends to investigate the influence of maximum ground acceleration; thus, peak ground acceleration (PGA) of available records was scaled to 0.2 g, 0.4 g, and 0.6 g.

As mentioned before, CFRDs are suitable for higher construction; therefore, the effect of dam height on the acceleration response and deformation characteristics should be investigated. Besides, other geometric properties as inclinations of upstream and downstream slopes, crest widths may affect the dam response. To investigate the

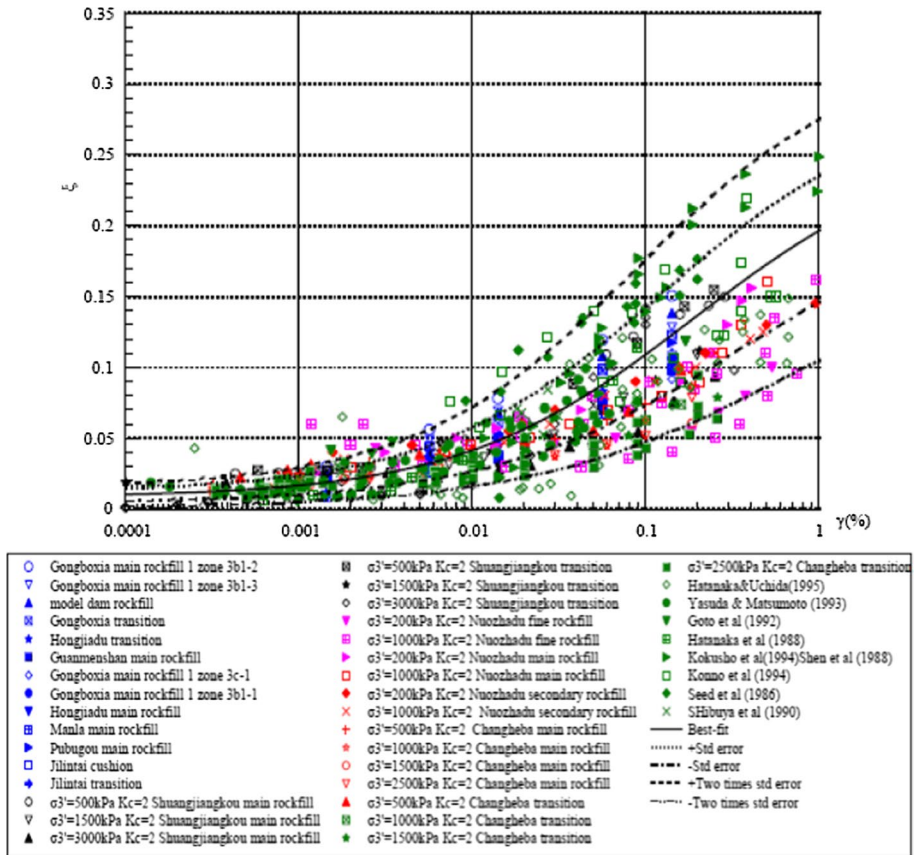


Fig. 7 Data points defining x versus g relationships for 35 kinds of rockfills based on testing along with the best-fit curve, \pm one standard division curves and two times standard division curves (Jia and Chi 2012)

Table 4 Material properties of dam models

Unit weight (γ) (kN/m ³)	Poisson's ratio (ν)	Cohesion (C) (kN/m ²)	Internal friction angle (ϕ) (°)
22	0.2	0	35°–40°–45°–50°

Table 5 Earthquakes used in the analyses

Earthquakes	Date	Fault mechanism	PGA	Predominant period(s)	Moment magnitude (M_w)
Cape Mendocino	1992	Thrust	0.39	0.24	7.2
Düzce	1999	Strike-slip	0.35	0.82	7.2
Kobe	1995	Strike-slip	0.50	0.44	6.9
Landers	1992	Strike-slip	0.65	0.08	7.3
Northridge	1994	Thrust	0.40	0.22	6.7
Tabas	1978	Thrust	0.11	0.54	7.4

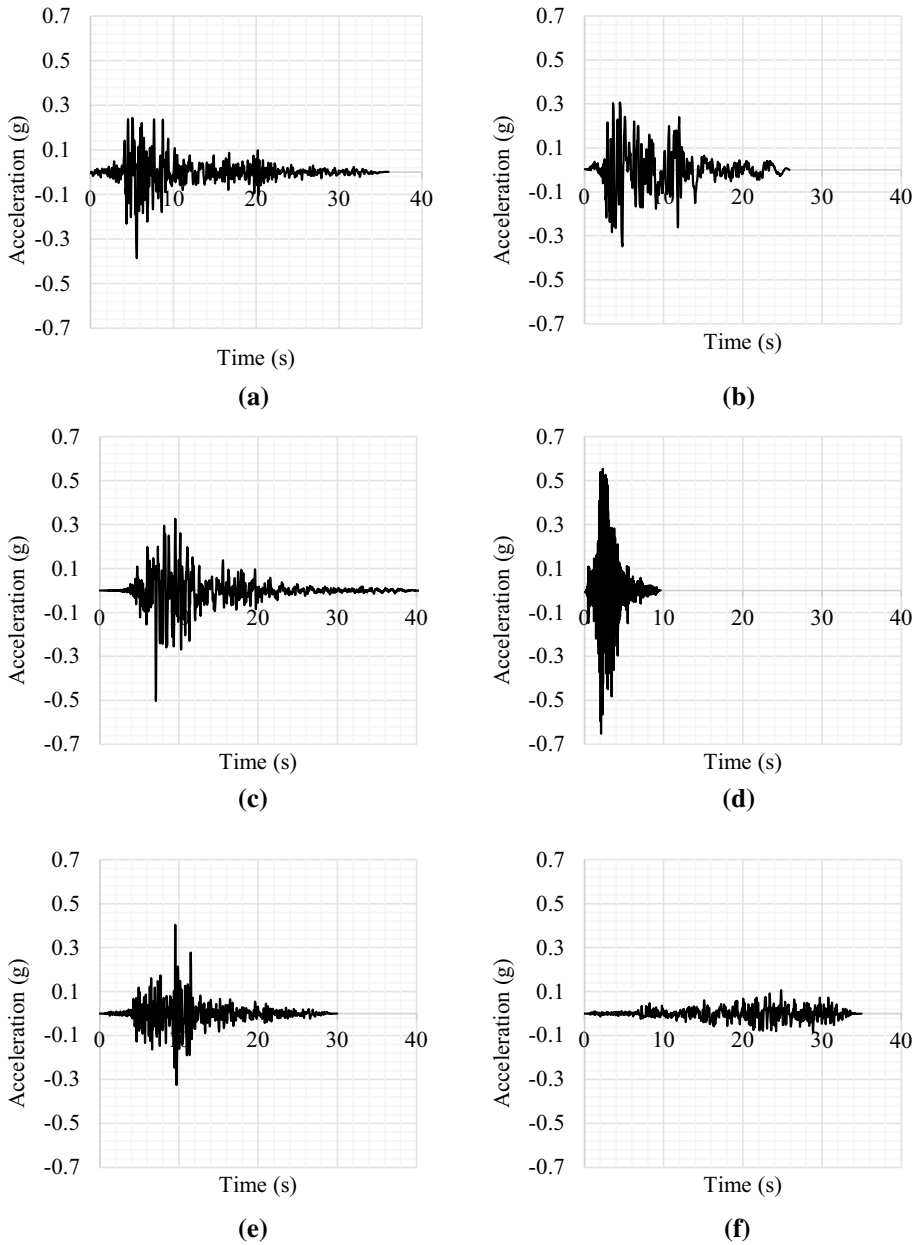


Fig. 8 Acceleration–time history of the earthquakes for 5% damping **a** Cape Mendocino, **b** Düzce, **c** Kobe, **d** Landers, **e** Northridge, **f** Tabas

existence of any relation between dam response and dam geometry, different geometric properties were tested. Table 6 shows the used parameters in dam models.

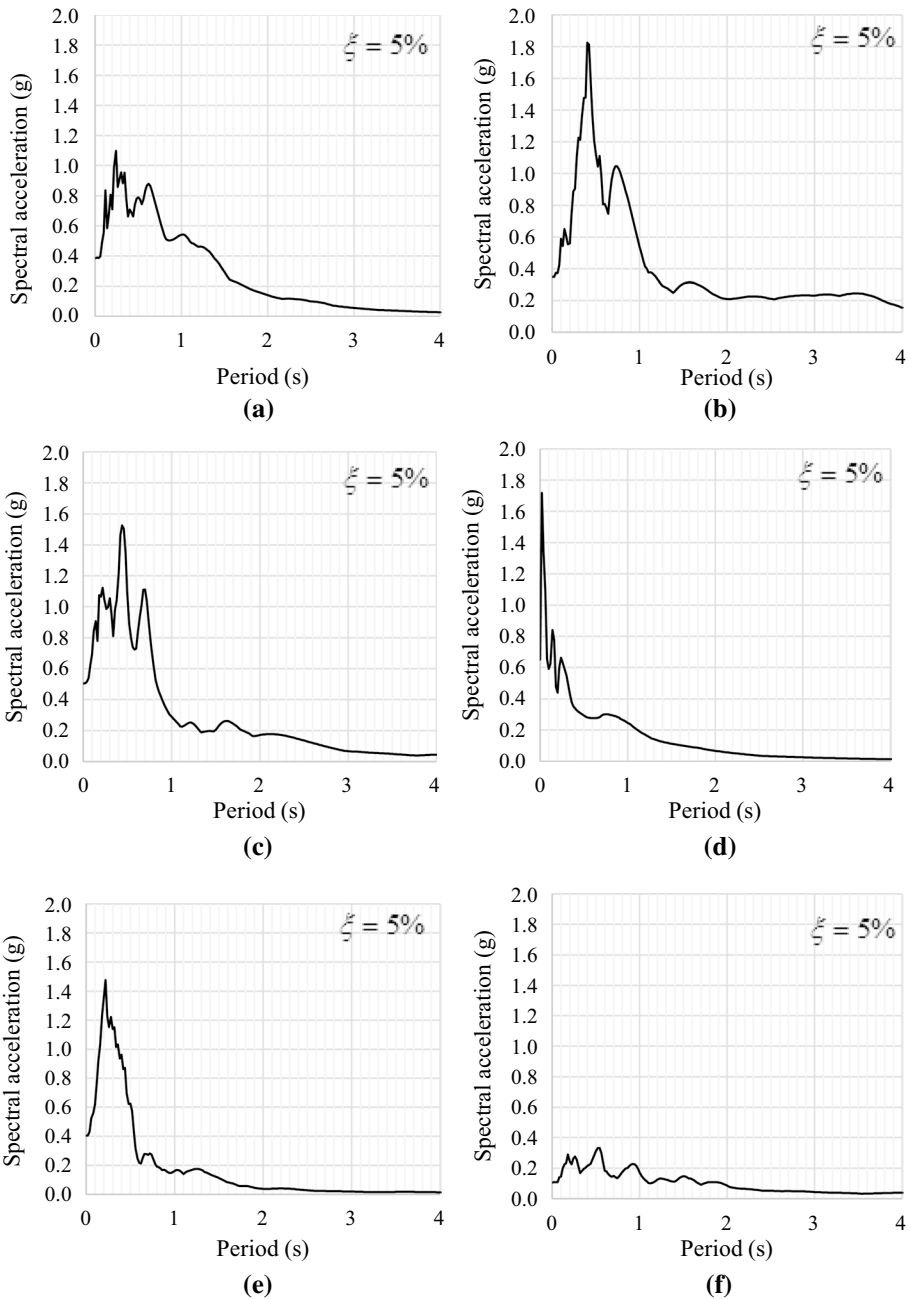


Fig. 9 Response spectrum of the earthquakes for 5% damping **a** Cape Mendocino, **b** Düzce, **c** Kobe, **d** Landers, **e** Northridge, **f** Tabas

Table 6 Used parameters in dam models

Dam height	50 m–100 m–150 m–200 m
Crest width	5 m–10 m–15 m–20 m
Slope inclination	1:1.2-1:1.4-1:1.6-1:1.8
Internal friction angle	35°–40°–45°–50°
Earthquake	6 records
Peak ground acceleration	0.2 g–0.4 g–0.6 g
Horizontal seismic coefficient	$a_{\max}/2$ – $a_{\max}/3$

4 Method of analysis

The simulation procedure of the study contains static, pseudo-static and dynamic analysis stages, respectively. Analyses were carried out for empty reservoir conditions; hence, the influence of hydraulic pressure was ignored. Since the initial static stress distribution of gravitational loads is required for the following equivalent linear analysis steps, static analyses of dam models were conducted firstly. Then, dynamic analyses were carried out applying the equivalent linear analysis procedure. QUAKE/W was used for both static and dynamic analyses.

Dynamic analysis procedure is listed as follows:

1. Static analysis

To observe the dynamic response of a dam, static analysis should be followed by a dynamic one. Gravitational load-induced stresses obtained from the static analysis are used to calculate effective stress-dependent dynamic parameters as cyclic stress ratio and shear modulus.

2. Input motion

Acceleration records of six actual earthquakes obtained from the PEER Strong Motion Database were applied to the dam models. Excitations were selected according to the frequency content, predominant period and moment magnitude range from 6.5 to 7.5 (Table 5).

3. Material properties

As summarized in Table 4, only one type of rock is used in models and, as noted before, damping and shear modulus degradation curves of fill material were defined to sight how the shear modulus and damping properties change during the earthquake and affect the dynamic response of dam. Besides, as seen in Eq. 4 (Hardin et al. 1972), maximum shear modulus depends on mean effective stress and effective stress changes with depth. Since the effective stress and maximum shear modulus show differences with depth, the dam body was divided into 10-m-thick equal layers and the maximum shear modulus was calculated at the midpoint of each layer, for a more accurate calculation.

$$G_{\max} = 3230 \times \frac{(2.973 - e)^2}{(1 + e)} \times \text{OCR}^K \times \sigma_m^{1/2} \quad (4)$$

In this equation, G_{\max} is maximum shear modulus, e is the void ratio, OCR is the over consolidation ratio, σ_m is the mean principle effective stress, and K is a constant and depends on the plasticity index, PI.

4. Mesh generation

This study contains 24 different numerical models and the number of mesh changes with the dimension of dam models. However, mesh generation was made according to the wavelength (λ). Kuhlemeyer and Lysmer (1973) proposed an equation for the mesh dimensions in terms of wavelength. For an accurate simulation, recommended mesh size (ΔL) should be less than one-tenth to one-eighth of the wavelength associated with the highest frequency component of the wave ($\Delta L \leq \lambda/10$ to $\lambda/8$). A finite element size in numerical models is equal to one-tenth of the wavelength with the highest frequency.

5. Dynamic analysis

By using initial stress distribution of static analysis, dynamic analyses were carried out and the acceleration histories were recorded at nodes. QUAKE/W enables to store the data of acceleration, velocity, displacement, strain, stress, and pore pressure. However, in this study, acceleration records are required for the permanent displacement calculations.

6. Permanent displacement calculation

Newmark's (1965) sliding block method was utilized in this study for the permanent displacement calculations. This method describes the sliding portion of the slope as a rigid block. This rigid block is free to move on an inclined slip surface linearly. Accordingly, a yield acceleration (k_y) is defined for the sliding block. This yield acceleration can be described as the maximum acceleration value in which the slope can withstand without any deformation, and can be determined from pseudo-static analysis. The pseudo-static analysis is a limit equilibrium-based method and used to analyze the dynamic stability of slopes. Roughly, earthquake-induced forces are multiplied with a coefficient and applied to the slope as they act horizontal constant forces. The pseudo-static analysis provides the factor of safeties of potential sliding surfaces. Herein, the factor of safety exhibits unity (FS = 1) for yield acceleration value of sliding part of the slope. According to Newmark's assumption, for the acceleration values more than yield acceleration, sliding portion of the slope exhibits permanent displacement until the relative velocity between the sliding portion and the ground reaches zero. Firstly, yield acceleration and earthquake-induced acceleration records are obtained for the pertinent sliding portion. Then, to evaluate permanent displacements, the cumulative differences of the acceleration values more than yield acceleration are integrated once with respect to time to obtain velocity–time history of the motion and this velocity–time history is integrated once again until the relative velocity becomes zero.

Complex geotechnical problems require simplifications for the preparation of numerical models and suggestions of applicable approaches for the solution. Many assumptions lay the foundation of this simplification; thus, some requisites may not be met. Therefore, the limitations of the applied method should be kept in mind. As utilized in the present study, limit equilibrium-based pseudo-static analysis and Newmark sliding block method are widely preferred ones for the seismic slope stability assessments. The limit equilibrium method assumes

the material to have rigid, perfectly plastic behavior and exhibit ductile deformation. However, many soil types show brittle and strain-softening characteristics (Kramer 1996). The strain-softening materials have two different stress levels as peak and residual shear strength. During the loading, the peak shear strength may not be reached simultaneously at every point of failure surface. Hence, shear strength decreases from peak to residual dramatically, and this initiates a shear stress redistribution to adjacent soil. Consequently, the distribution of deviatoric stresses may enlarge the failure zone until the slope fails. Therefore, the residual shear strength of material should be used for the calculations while analyzing the strain-softening material with the limit equilibrium method. Likewise, the pseudo-static analysis method is not capable to evaluate weakening type (flow liquefaction and cyclic mobility) stability problems; thus, it is important to be careful while utilizing pseudo-static analyses for the soils that generate large pore water pressures or shear strength degradation exceeds 15% (Kramer 1996).

5 Discussion of the results

Numerically evaluated results were normalized with maximum ground acceleration, and the influence of the slope inclination on the acceleration response of rockfill dams shown in Fig. 10 is interpreted in terms of variation of normalized acceleration along the centerline of the dam body. As seen in the given figures, different slopes follow nearly the same path for all dam heights; however, an increment in acceleration amplification can be observed with increasing dam height. Although the higher dams with steeper slopes exhibit more amplification at the crest, the effects of slope inclination appear to be minor.

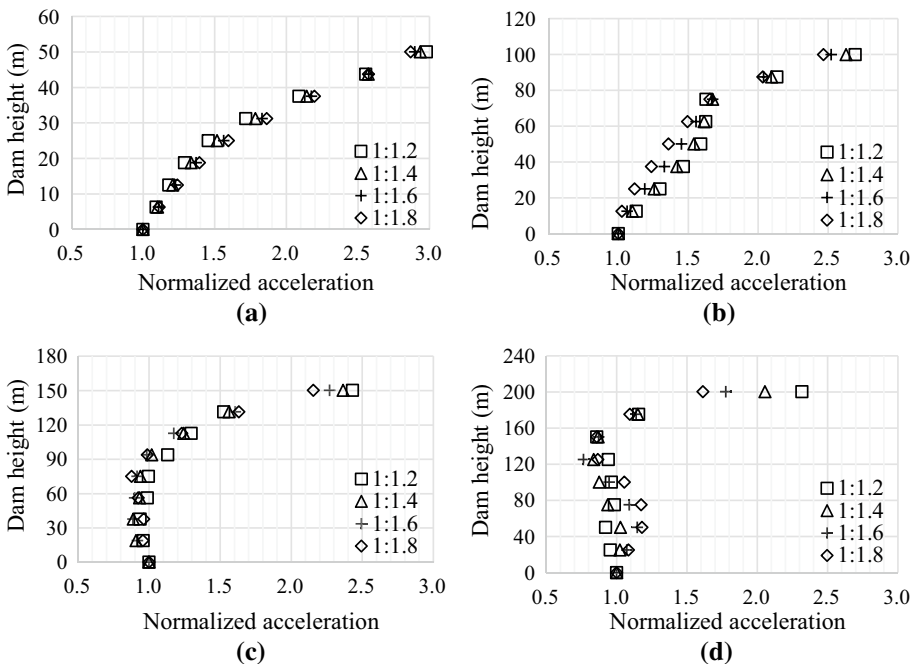


Fig. 10 Effect of slope inclination on the variation of normalized acceleration along the dam height for **a** 50 m, **b** 100 m, **c** 150 m, **d** 200 m

As is known from previous studies, the dynamic response of dams is mostly dominated by the properties of input motion as peak ground acceleration, duration and frequency of motion. To investigate these findings, dam models with the same properties were tested under different peak ground acceleration values as 0.2 g, 0.4 g, and 0.6 g for each dam height. Obtained normalized acceleration results are plotted in Fig. 11 against the dam height, and according to the figures, acceleration amplifications decrease with increasing PGA and dam height. The existence of this reverse proportion can be explained with the natural period of the dam. The higher dams have higher periods, and they expose a flexible behavior under dynamic loading. Similarly, PGA increment increases the strain, and correspondingly, the transmissibility of the waves through the dam body decreases. Consequently, while shear modulus decreases with increasing strain and PGA, the damping of fill material increases.

Herein, when all these figures are considered, a remarkable behavioral difference is realized at dam crest. Indiscriminately, variation of acceleration amplifications shows a dramatic increment around 1/4 of dam height from the top for all dam models. Thus, this region exhibits more displacement than the remaining part of the dam body, and additional structural treatments are required for this part as reinforcing with geogrids, as previously proposed by Liu et al. (2014).

Although the post-construction deformations of CDRDs are generally triggered by several mechanisms (weathering of fill material, face slab failure, reservoir fluctuation, etc.), only the earthquake caused deformations are investigated in this paper. As mentioned before, the Newmark method is utilized to evaluate the deformations and

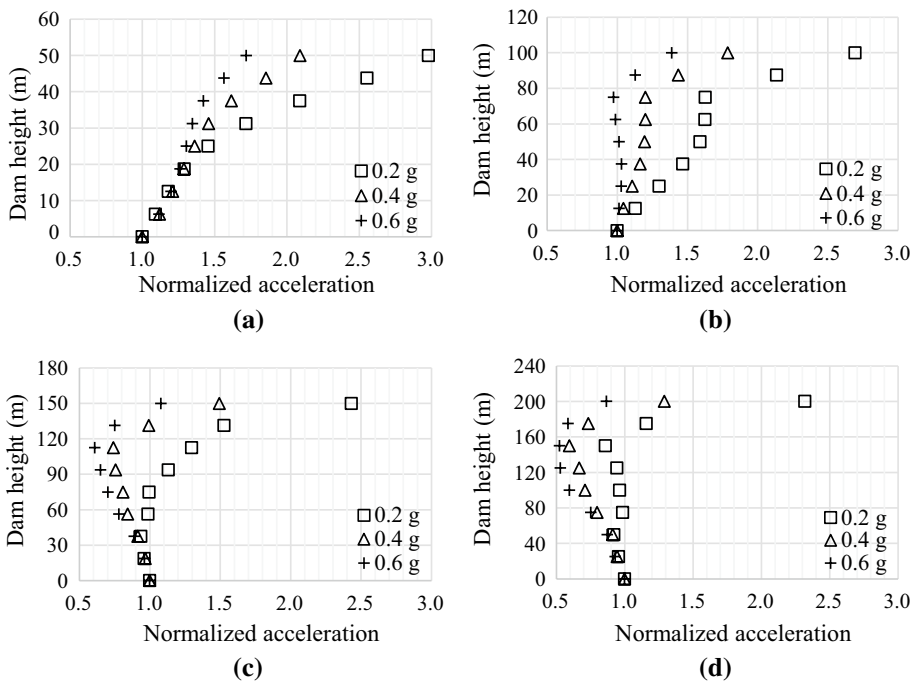


Fig. 11 Effect of maximum ground acceleration on the variation of normalized acceleration along the dam height for **a** 50 m, **b** 100 m, **c** 150 m, **d** 200 m dam

this method requires yield acceleration and earthquake-induced accelerations. Besides, earthquake-induced accelerations are affected by the natural period of dam and frequency of input motion. Under these circumstances, revealing the contribution of yield acceleration, maximum crest acceleration, and peak ground acceleration to permanent displacement could be useful. Thus, Fig. 12 is plotted for the variation of permanent displacement against the ratio of yield acceleration to maximum crest acceleration. Although the data are widely scattered, a solid line can be drawn for the average values and these values can be utilized for practical evaluations. As is seen obviously, CFRDs exhibit larger deformations for the smaller values of the yield acceleration and crest acceleration ratio. If this ratio is larger than 0.4, deformations may fall into the safe limit which is smaller than 10 cm.

In Fig. 13, the variation of permanent displacement is given in terms of normalized acceleration values. Maximum ground acceleration is used for the normalization of yield acceleration. Limit values of permanent displacement and normalized acceleration are demonstrated with the solid lines. Considering these indicators, likely permanent displacement may not exceed the limits if the ratio of yield acceleration to peak ground acceleration is larger than 0.4. Moreover, when this ratio exceeds unity, permanent displacements will most probably be smaller than 10 cm.

Even the suggested relations of this numerical study were constructed utilizing the models of rockfill dams, available case histories of different dams may be utilized to increase the reliability of the proposed information. Thus, 37 case studies of various embankments including multi-zone (type 1), multi-zone rockfill (type 2), concrete-faced rockfill (type 3),

Fig. 12 Variation of permanent displacement with the ratio of a_{yield}/a_{crest}

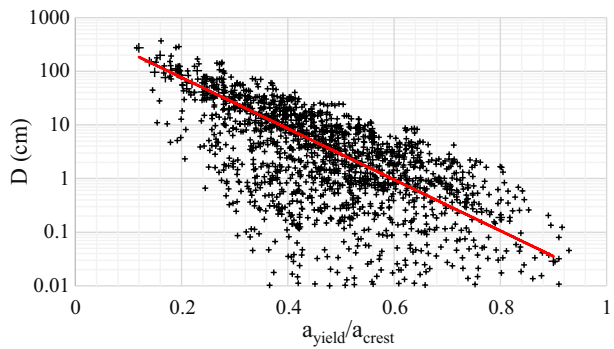
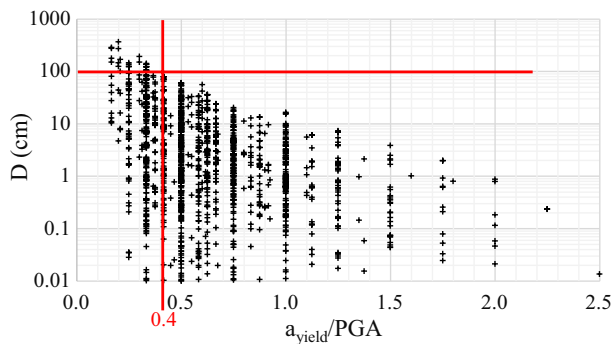


Fig. 13 Variation of permanent displacement with the ratio of a_{yield}/PGA for all dam heights



and concrete-faced decomposed granite or gravel (type 4) dams were reevaluated with the given relations for comparisons. The properties of dams and causative earthquakes and the damages due to the dynamic loading are summarized in Table 7. Numerically obtained deformations are expressed in terms of minimum and maximum horizontal displacements in the “numerical displacement” column of the table. The real displacements observed in the dam site are given in the “observed displacements” column of the table. Owing to the large variety in the dam heights of case studies, yield acceleration of dams (a_{yield}) is normalized with maximum ground acceleration of the input motion (PGA) and this $a_{\text{yield}}/\text{PGA}$ ratio is used for the comparisons. Herein, researchers noted that the used maximum ground acceleration of the input motion values was obtained utilizing the attenuation relationships due to the lack of instrumentation at dam sites. Hereby, used parameters are T_p for predominant period of the earthquake, T_D (s) for fundamental period of the dam, PGA (g) for peak ground acceleration of input motion at dam site obtained with attenuation relations, M_w for moment magnitude of the earthquake, a_y (g) for yield acceleration. In Fig. 14, numerically evaluated results are given with the observed displacements. The average values of the numerical results are also shown in the figure. Since type 1 (the multi-zone type) dams are mostly composed of earth fill, their results expressed with a different marker and the results appear to be scattered differently. The main reason for this behavior may be the Newmark sliding block method. Jibson (1993) summarizes the limitation of this method. Newmark’s method is unable to model the flexibility of the materials, and postulates of the proposed method generally are valid for compacted or overconsolidated clays and very dense or dry sands. Similar to the limit equilibrium, Newmark assumes the sliding block as rigid and the behavior is perfectly plastic. This assumption can be valid when a stiff soil is subjected to low frequency and generates long wavelength. Unlikely, exposure of soft soil to high frequency leads short wavelengths and this causes oppositely oriented inertial forces through the slope. Due to the variation of the directions, the resultant force will be underestimated. Besides, this method excludes the strain-hardening and strain-softening materials. Since the yield acceleration will not remain the same during the motion and change with the slope deformation, permanent displacement of strain-softening materials will be underestimated, while strain-hardening materials are overestimated. Similarly, due to their rockfill content, results of both type 2 (multi-zone rockfill), type 3 (concrete-faced rockfill) and type 4 (concrete-faced decomposed granite or gravel) dams are expressed with the same marker. When the numerical and measured deformations are compared, the results of rockfill type dams are quite compatible with each other. However, the evaluated numerical displacements vary in a wide range. As stated before, although obtained earthquake-induced permanent displacements are directly related to yield acceleration, the Newmark sliding block method is a well-established method for the calculation of permanent displacements. However, the evaluation of yield acceleration includes both determinations of yield coefficient of possible slip surface and consideration of all possible accelerations; hence, these steps can be said to be quite confusing and are possible sources of errors. Although there are logical approaches for the selection of yield coefficient, there is still no clear consensus.

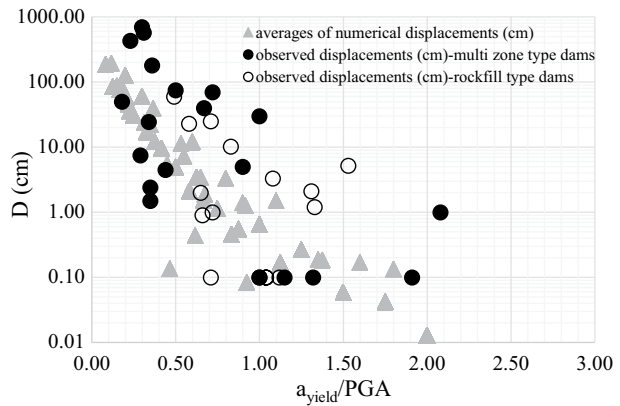
Table 7 Properties of case studies

Dam	Earthquake						α_y /PGA	Observed Displacement	Numerical Displacement	References			
	Type	Height (m)	i_D (s)	α_y (g)	Date	M_w					PGA (g)	Distance (km)	T_p (s)
Kitayama	1	25	0.34	0.15	17.01.1995	7.1	0.3	31	0.32	0.5	75	0.01–60	Sakamoto et al. (2002)
Makubetsu	1	26.9	0.42	0.18	26.09.2003	8	0.25	141	0.5	0.72	70	0.01–30	Nagayama et al. (2004)
Otani-Ike	1	27	0.65	0.15	21.12.1946	8.3	0.8	45	0.32	0.19	0	0.4–400	Stroitel (1969)
Chofukujji	1	27.2	0.38	0.09	23.10.2004	6.8	0.1	21	0.32	0.9	5	0.01–10	Yasuda et al. (2005)
Yamam regulatory	1	27.2	0.38	0.1	23.10.2004	6.8	0.55	7	0.32	0.18	50	0.4–400	Yasuda et al. (2005)
Brea	1	27.4	0.76	0.25	17.01.1994	6.9	0.19	67	0.45	1.32	0.1	0.01–4	Abdel-Ghaffar and Scott (1979)
Hebgen	1	27.5	0.47	0.22	17.08.1959	7.5	0.7	100	0.65	0.31	576	0.7–110	Seed et al. (1978)
Rudramata	1	27.6	0.28	0.07	26.01.2001	7.6	0.3	80	0.55	0.23	433	2–600	Singh et al. (2007)
EJ Chesbro	1	29	0.46	0.15	17.10.1989	7	0.43	13	0.32	0.35	1.5	0.2–70	Harder (1991)
Tokiwa	1	33.5	0.49	0.2	17.01.1995	7.1	0.2	10	0.32	1	0.1	0.01–20	Matsumoto et al. (1996)
Ono	1	36.6	0.52	0.27	01.09.1923	8.2	0.8	96	0.6	0.34	24.4	0.2–70	Seed et al. (1978)
Long Valley	1	38.4	0.52	0.23	27.05.1980	6.1	0.2	16	0.25	1.15	0.1	0.01–6	Lai and Seed (1985)
Murayama	1	39	0.52	0.29	09.01.1923	8.2	0.8	96	0.6	0.36	180	0.01–90	Seed et al. (1978)
Kawanishi	1	43	0.59	0.14	23.10.2004	6.8	0.14	17	0.32	1	30	0.01–10	Yasuda et al. (2005)
Guadalupe	1	43.3	0.68	0.19	17.10.1989	7	0.43	19	0.32	0.44	4.5	0.02–12	Harder (1991)
LA dam	1	47.3	0.6	0.15	17.01.1994	6.9	0.43	7	0.32	0.35	2.4	0.2–70	Seed et al. (1978)
Asagawara regulatory	1	56.4	0.53	0.08	23.10.2004	6.8	0.12	24	0.32	0.67	40	0.02–30	Yasuda et al. (2005)
Lexington	1	62.5	0.77	0.13	17.10.1989	7	0.45	10	0.32	0.29	7.5	0.6–200	Harder (1991)
Baihe	1	66	0.89	0.06	28.07.1976	7.8	0.2	150	0.52	0.3	700	0.9–110	Lingyao et al. (1980)

Table 7 (continued)

Dam	Earthquake				α_y /PGA	Observed Displacement	Numerical Displacement	References					
	Type	Height (m)	i_D (s)	α_y (g)									
Name	Type	Height (m)	i_D (s)	α_y (g)	Date	M_w	PGA (g)	Distance (km)	T_p (s)	D (cm)	D (cm)	$D_{min}-D_{max}$	References
Guldurecek	1	68	0.91	0.27	06.06.2000	5.9	0.13	19	0.27	2.08	1	0.02–1	Ozkan et al. (1996)
Oroville	1	235	2.74	0.21	08.01.1975	6	0.11	7	0.25	1.91	0.1	0.02–1.5	Bureau et al. (1985)
San Justo	2	41	0.51	0.27	17.10.1989	7	0.26	27	0.32	1.04	0.1	0.01–10	Harder (1991)
Shin-Yamam.	2	44.5	0.56	0.36	23.10.2004	6.8	0.55	6	0.32	0.65	2	0.1–35	Yasuda et al. (2005)
Surgu	2	55	0.72	0.15	05.05.1986	6.6	0.21	10	0.32	0.71	0.1	0.01–30	Ozkan et al. (1996)
Newell	2	55.5	0.75	0.25	17.10.1989	7	0.43	10	0.32	0.58	23	0.8–60	Harder (1991)
La Villita	2	60	0.94	0.2	11.10.1975	4.9	0.15	52	0.27	1.33	1.2	0.02–4	Elgamal et al. (1990)
La Villita	2	60	0.94	0.2	19.09.1985	8.1	0.24	58	0.48	0.83	10.2	0.04–11	Elgamal et al. (1990)
Anderson	2	71.6	1.08	0.27	24.04.1984	6.2	0.41	16	0.32	0.66	0.9	0.1–35	Bureau et al. (1985)
Anderson	2	73.2	1.08	0.34	17.10.1989	7	0.26	16	0.32	1.31	2.1	0.02–4	Harder (1991)
Matahina	2	86	1.08	0.17	02.03.1987	6.5	0.24	11	0.28	0.71	25	0.01–30	Pender and Robertson (1987)
Takami	2	120	1.31	0.37	26.09.2003	8	0.33	140	0.5	1.12	0.1	0.01–10	Nagayama et al. (2004)
Miboro	2	131	1.43	0.23	19.08.1961	7	0.15	16	0.32	1.53	5.2	0.09–4	Bureau et al. (1985)
El Infernillo U/S	2	148	1.58	0.13	21.09.1989	7.2	0.12	116	0.56	1.08	3.3	0.01–6	Resendiz et al. (1982)
Kalpong	3	27	0.35	0.1	14.09.2002	6.5	0.1	21	0.27	1	0.1	0.01–10	Rai and Murty (2003)
Ishibuchi	3	53	0.63	0.28	26.05.2003	7.1	0.27	85	0.42	1.04	0.1	0.01–10	Nagayama et al. (2004)
Zipingpu	3	156	0.21	0.27	12.05.2008	7.9	0.55	17	–	0.49	60	0.01–75	Kan et al. (2017)
El Khattabi	4	27.5	0.37	0.18	24.02.2004	6.4	0.25	21	0.25	0.72	1	0.05–25	EERI (2004)

Fig. 14 Comparison of numerical and observed permanent displacement with the ratio of a_{yield}/PGA



6 Conclusion

Concrete-faced rockfill dams are increasingly preferred and distributed all around the world according to the report of International Commission on Large Dams (ICOLD 2004), at especially highly seismic regions, owing to their economic benefit of using nearby material, high adaptation to local site conditions (geological and geophysical), and capability of withstanding strong ground motions. Since thoroughly designed and elaborately constructed dams exhibit satisfactory performance during the earthquake, the dynamic behavior of rockfill material and design criteria of CFRDs must be established clearly. This paper intends to contribute to the identification of dynamic responses of CFRDs by conducting a series of numerical analyses. The conclusions of the study are summarized below.

1. Conduction of numerical analyses requires suitable software. Thus, selected software was validated utilizing the dynamic response results of Sürgü Dam after the Malatya earthquake. Numerically evaluated seismic performance of the mentioned dam in terms of permanent deformations and acceleration amplifications are coherent with the site measurements.
2. The existence of any relation between the slope inclination and seismic response of the dam was scrutinized. Earthquake-induced accelerations draw the same patterns along the dam body for almost all analyses. However, the influence of slope inclination becomes perceivable as the dam height increases and steeper slopes cause slightly more amplification. Even so, the acceleration response of CFRDs can be said to be less sensitive to the inclination of slope.
3. The amplification of the acceleration decreases with increasing dam height and PGA. Damping of the fill material and natural period of the dam can be responsible for this decrement. There is a direct proportion between strain and damping. The higher PGA values increase the strain and accordingly damping increases. Hence, earthquake occasioned energy will be absorbed by the fill material, and amplifications decrease. Besides, the natural period increases with dam height, and consequently, higher frequencies are attenuated.
4. When the acceleration responses were examined, abruptly increased amplifications were observed around the crest of dam models. The region rests between the crest and the 3/4 height of the dam from bottom amplifies the accelerations more than the remaining

- part. Thus, this remarkable increment may require additional reinforcement for the upper part of the dam as a prevention for the excessive strains that can jeopardize the overall stability.
5. According to the numerical results, when the ratio of the yield acceleration to the peak ground acceleration is larger than 0.4; the ratio of the yield acceleration to the crest acceleration is larger than 0.3, and envisioned seismically induced permanent displacements can be below the safety limits.
 6. According to the acceleration and permanent displacement responses of dam models, earthquake parameters are the most significant components which may bring the dam to the brink of the instability.
 7. Deformation results of 37 case studies were utilized for the assessment of numerically obtained deformations. The comparison results of measured and predicted deformations are quite consistent with each other for 16 rockfill type dams. However, multi-zone type dams include earthfill, and their numerical results are not compatible with the observed ones. Newmark's method ignores the flexible behavior of material, and variation of yield acceleration during the motion due to the slope deformation. Moreover, a 3D behavior is treated as a 2D plain-strain deformation problem with this approach. Therefore, a wide range of numerical deformation is evaluated for a specified value of $a_{\text{yield}}/\text{PGA}$ and permanent displacement of strain-softening materials (multi-zone type dams) is underestimated, while strain-hardening materials are overestimated. This study includes a comprehensive investigation on the dynamic response of the CFRDs with the aim of elucidating the influence of different parameters. Engineers may utilize the outputs of this study at the preliminary design step of CFRDs for the quick estimation of likely residual deformations with acceptable certainty as a practical perspective.

References

- Abdel-Gbaffar AM, Scott RF (1979) Analysis of earth dam response to earthquakes. *J Geotech Eng Div* 105(12):1379–1404
- Ambraseys NN, Menu JM (1988) Earthquake-induced ground displacements. *J Earthq Eng Struct Dyn* 16:985–1006
- Bray JD (2007) Simplified seismic slope displacement procedures. In: Pitilakis KD (ed) *Earthquake geotechnical engineering*. Springer, Dordrecht, pp 327–353
- Bray JD, Travararou T (2007) Simplified procedure for estimating earthquake-induced deviatoric slope displacements. *J Geotech Geoenviron Eng* 133(4):381–392
- Bray JD, Augello AJ, Leonards GA, Repetto PC, Byrne RJ (1995) Seismic stability procedures for solid-waste landfills. *J Geotech Eng* 121(2):139–151
- Bureau G, Volpe RL, Roth WH, Udaka T (1985) Seismic analysis of concrete face rockfill dams. In: *Concrete face rockfill dams—design, construction, and performance*. ASCE, pp 479–508
- Chen S, Han H (2009) Impact of the “5.12” Wenchuan earthquake on Zipingpu concrete face rock-fill dam and its analysis. *Geomech Geoeng* 4(4):299–306
- Earthquake Engineering Research Institute (2004) Preliminary observation on the Al Hoceima Morocco earthquake of 24 February, 2004. Special report EERI, Oakland, CA, USA
- Elgamal AW, Scott RF, Succarieh MF (1990) La Villita dam response during five earthquakes including permanent deformation. *J Geotech Eng* 114:1443–1462
- Fu Z, Chen S, Wang T (2017) Predicting the earthquake-induced permanent deformation of concrete face rockfill dams using the strain-potential concept in the finite-element method. *Int J Geomech* 17(11):04017100
- Harder LH Jr (1991) Performance of earth dams during Loma Prieta earthquake. *US Geol Surv Prof Pap* 1552:3–26

- Hardin BO, Drnevich VP (1972) Shear modulus and damping in soils: design equations and curves. *J Soil Mech Found Div* 98:sm7
- Huang D, Wang G, Du C, Jin F, Feng K, Chen Z (2020) An integrated SEM-Newmark model for physics-based regional coseismic landslide assessment. *Soil Dyn Earthq Eng* 132:106066
- Hynes-Griffin ME, Franklin AG (1984) Rationalizing the seismic coefficient method. Misc. Paper No. GL-84-13, U.S. Army Engr. WES, Vicksburg, MS
- ICOLD (International Committee on Large Dams) (2004) Concrete face rockfill dams concepts for design and construction
- Javdanian H, Pradhan B (2019) Assessment of earthquake-induced slope deformation of earth dams using soft computing techniques. *Landslides* 16(1):91–103
- Jia YF, Chi SC, (2012) Application of rockfill dynamical characteristic statistic curve in mid-small scale concrete face dam dynamic analysis. In: 15th world conference on earthquake engineering, Lisbon, pp 24–28
- Jibson RW (1993) Predicting earthquake-induced landslide displacements using Newmark's sliding block analysis. *Transp Res Rec* 1411:9–17
- Jibson RW (2007) Regression models for estimating coseismic landslide displacement. *Eng Geol* 91(2):209–218
- Kan ME, Taiebat H, Taiebat M (2017) A framework to assess Newmark-type simplified methods for evaluation of earthquake-induced deformation of embankments. *Can Geotech J* 54(3):392–404
- Kramer SL (1996) Geotechnical earthquake engineering. Prentice-hall civil engineering and engineering mechanics series. Prentice Hall, Upper Saddle River, p 673
- Kramer SL, Smith MW (1997) Modified Newmark model for seismic displacements of compliant slopes. *J Geotech Geoenviron Eng* 123(7):635–644
- Kuhlmeyer RL, Lysmer J (1973) Finite element method accuracy for wave propagation problems. *J Soil Mech Found Div ASCE* 99(5):421–427
- Lai SS, Seed HB (1985) Dynamic response of Long Valley Dam in the Mammoth Lake earthquake series of May 25–27, 1980 (No. 142304). College of Engineering, University of California
- Leshchinsky BA (2018) Nested newmark model to calculate the post-earthquake profile of slopes. *Eng Geol* 233:139–145
- Lin JS, Whitman RV (1986) Earthquake induced displacements of sliding blocks. *J Geotech Eng* 112(1):44–59
- Lingyao L, Kueifen L and Dongping B (1980) Earthquake damage of Baihe earth dam and liquefaction characteristics of sand and gravel materials. In: Proceeding of the 7th world conference on earthquake engineering, İstanbul, Turkey, September, pp 8–13
- Liu J, Liu F, Kong X, Yu L (2014) Large-scale shaking table model tests of aseismic measures for concrete faced rock-fill dams. *Soil Dyn Earthq Eng* 61:152–163
- Liu J, Liu F, Kong X, Yu L (2016) Large-scale shaking table model tests on seismically induced failure of concrete-faced rockfill dams. *Soil Dyn Earthq Eng* 82:11–23
- Makdisi FI, Seed HB (1978) Simplified procedure for estimating dam and embankment earthquake induced deformations. *J Geotech Eng* 104(7):849–867
- Marandi SM, Vaezi Nejad SM, Khavari E (2012) Prediction of concrete faced rock fill dams settlements using genetic programming algorithm. *Int J Geosci* 3(3):601
- Matsumoto N, Nakamura A, Sasaki T, Iwashita T (1996) Effects on dams. *Soils Found* 36:273–281
- Meehan CL, Vahedifard F (2013) Evaluation of simplified methods for predicting earthquake-induced slope displacements in earth dams and embankments. *Eng Geol* 152(1):180–193
- Nagayama I, Yamaguchi Y, Sasaki T, Nakamura A, Kawasaki H, Hirayama D (2004) Damage to dams due to three large earthquakes occurred in 2003 Japan. In: 36th Joint meeting panel on wind and seismic effects
- Newmark NM (1965) Effects of earthquakes on dams and embankments. *Géotechnique* 15:139–160
- Özkan MY, Erdik M, Tuncer MA, Yılmaz C (1996) An evaluation of Sürgü dam response during 5 May 1986 earthquake. *Soil Dyn Earthq Eng* 15(1):1–10
- Pang R, Xu B, Kong X, Zou D (2018) Seismic fragility for high CFRDs based on deformation and damage index through incremental dynamic analysis. *Soil Dyn Earthq Eng* 104:432–436
- Pender MJ, Robertson TW (1987) Edgecumbe earthquake: reconnaissance report. *Earthq Eng Res Inst* 20:201–249
- Rai DC, Murty CVR (2003) Reconnaissance report on North Andaman (Diglipur) earthquake of 14 September 2002. Department of Civil Engineering Indian Institute of Technology Kanpur, Kanpur, p 208016
- Rathje EM, Saygili G (2009) Probabilistic assessment of earthquake-induced sliding displacements of natural slopes. *Bull N Z Soc Earthq Eng* 42(1):18

- Resendiz D, Romo MP, Moreno E (1982) El infiernillo and la villita dams: seismic behavior. *J Geotech Geoenviron Eng* 108:ASCE16791
- Roy R, Ghosh D, Bhattacharya G (2016) Influence of strong motion characteristics on permanent displacement of slopes. *Landslides* 13(2):279–292
- Sakamoto S, Yoshida H, Yamaguchi Y, Satoh H, Iwashita T, Matsumoto N (2002) Numerical simulation of sliding of an earth dam during the 1985 Kobe earthquake. In: *Proceeding of the 3rd US Japan workshop on advanced research on earthquake engineering for dams*, San Diego, CA, pp 22–23
- Saygılı G, Rathje EM (2008) Empirical predictive models for earthquake-induced sliding displacements of slopes. *J Geotech Geoenviron Eng* 134(6):790–803
- Seed HB (1979) Considerations in the earthquake-resistant design of earth and rockfill dams. *Geotechnique* 29(3):215–263
- Seed HB, Makdisi IF, De Alba P (1978) Performance of earthen dams during earthquakes. *J Geotech Eng* 104:967–994
- Sherard JL, Cooke JB (1987) Concrete-face rockfill dam: I assessment. *J Geotech Eng* 113(10):1096–1112
- Singh R, Roy D, Das D (2007) A correlation for permanent earthquake-induced deformation of earth embankments. *Eng Geol* 90(3–4):174–185
- Stroitel G (1969) Design and investigation of seismically stable dams in Japan. *Power Technol Eng (Formerly Hydrotech Construct)* 3:946–955
- Swaigood JR (2003) Embankment dam deformations caused by earthquakes. In: *7th Pacific conference on earthquake engineering*. University of Canterbury, Christchurch, New Zealand, pp 13–15
- Wang G (2012) Efficiency of scalar and vector intensity measures for seismic slope displacements. *Front Struct Civil Eng* 6(1):44–52
- Wang J, Yang G, Liu H, Nimbalkar SS, Tang X, Xiao Y (2017) Seismic response of concrete-rockfill combination dam using large-scale shaking table tests. *Soil Dyn Earthq Eng* 99:9–19
- Wang MX, Huang D, Wang G, Li DQ (2020) SS-XGBoost: a machine learning framework for predicting newmark sliding displacements of slopes. *J Geotech Geoenviron Eng* 146(9):04020074
- Yasuda N, Kondo M, Sano T, Yoshioka H, Yamaguchi Y, Sasaki T, Tomita M (2005) Effect of the mid Niigata prefecture earthquake in 2004 on dams. In: *37th Joint meeting, panel on wind and seismic effects*. US Japan Natural Resources Development Program, Technical Report

Publisher's Note Springer Nature remains neutral with regard to jurisdictional claims in published maps and institutional affiliations.